Periodic Branched Structures in a Phase-Separated Magnetic Colloid

Hao Wang,[1] Yun Zhu,[1] C. Boyd,[1] Weili Luo,[1,*] A. Cebers,[2] and R. E. Rosensweig[3]
[1]*Department of Physics, University of Central Florida, Orlando, Florida 32816*
[2]*Latvian Academy of Science, Riga, Latvia*
[3]*Exxon Research and Engineering Company, Annandale, New Jersey 08801*
(Received 22 November 1993)

Periodic branched columns are observed for the first time in a layer of phase-separated magnetic colloid confined in a cell. The periodicity λ scales with the layer thickness L. In the thin limit, where no branching occurs, $\lambda \propto L^{1/2}$. In the thick limit, each column develops a tree structure with branches and roots, and the columns are separated by shrubs while the scaling relation crosses over to $\lambda \propto L^{2/3}$.

PACS numbers: 75.50.Mm, 47.54.+r

Periodic structures in nature are often the optimum results of competition among different energies. Domain structure with alternating spin orientations in a ferromagnetic thin slab originates from the competition between the short range exchange interaction and the long range dipole energy [1]. The mechanism responsible for labyrinth patterns in ferrofluids [2] is the competition between the surface tension and the dipole interaction. The balance among various energy scales usually leads to scaling laws between different physical quantities.

In this Letter we report our studies of the periodic column structures in a phase-separated magnetic colloid when it is subjected to a magnetic field. For a thin cell, the columns are unbranched with the periodicity, λ, increasing with the cell thickness, L, as $\lambda \sim L^{1/2}$. For large L, we observed, for the first time in a magnetic colloid, multilevel branched fine structures in each column and dangling side branches between main columns. The scaling law relating the average distance between columns and the cell thickness then changes to $\lambda \sim L^{2/3}$. Although the unbranched columns in the thin limit have been seen before [3], the observations of multilevel branching, dangling side bands, scaling laws, and the connection between the structural change and the exponent's crossover are new. We will also show that contrary to the situations in 2D ferromagnets [1,4], different energies competing with each other originate from the same interaction, namely, the dipole interaction alone.

Experiments are performed for a magnetic colloid made of magnetite particles coated with oleic acid and suspended in *n*-eicosane (melting point: 309 K). The volume fraction of magnetic particles is 12% with mean diameter of particles 89 Å. Three kinds of sample cells are used: (a) parallel glass plates with plastic spacers (type *A*); (b) wedged glass plates with an angle between them of less than 1 deg (type *B*); and (c) tube with ellipsoidal cross section and the diameter of the tube gradually increasing from one end to the other (type *C*). Wedged cells make the thickness an adjustable parameter while a tube cell provides a clear side view. Melted sample is introduced to the gap of the cell by capillary effect. All the experimental results are obtained with the sample in the liquid phase. The magnetic field applied is generated by an electromagnet. The images of the structures are obtained by a charge-coupled device (CCD) camera connected to a microscope and recorded by a VCR. The heat generated by the microscope lamp is enough to melt the sample. The temperature gradient is less than 0.1 °C across the field of view.

In zero applied field (the residual due to the earth's magnetic field is 0.5 G), we observed large aggregates in the melted phase. The size of the aggregate droplets is much larger than the size of the magnetic particles. We believe that phase separation occurred in the system. Upon applying a magnetic field, the agglomerates break up into smaller droplets to decrease the demagnetizing field. At small layer thickness, L, the stable structure is a periodic two-dimensional lattice shown in Fig. 1 as observed from the top of the parallel plates. The magnetic field applied is 300 G, with orientation perpendicular to the surface of the sample cell. Each circular dot in Fig. 1 represents a cross section of a column with its long axis parallel to the field direction. The separation between the

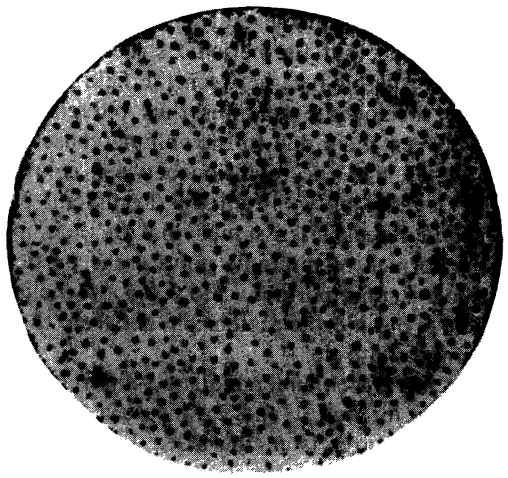

FIG. 1. Periodic lattice structure in a field of 300 G. The thickness L is less than 2 μm.

0031-9007/94/72(12)/1929(4)$06.00

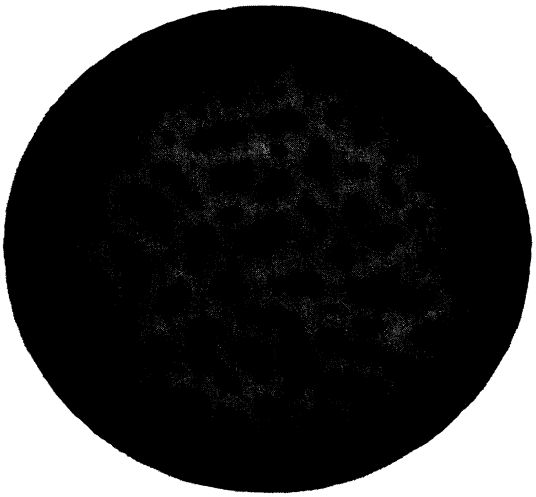

FIG. 2. Periodic pattern in a relatively thick cell. The thickness $L = 25$ μm. The cross sections are altered from their original circular geometry.

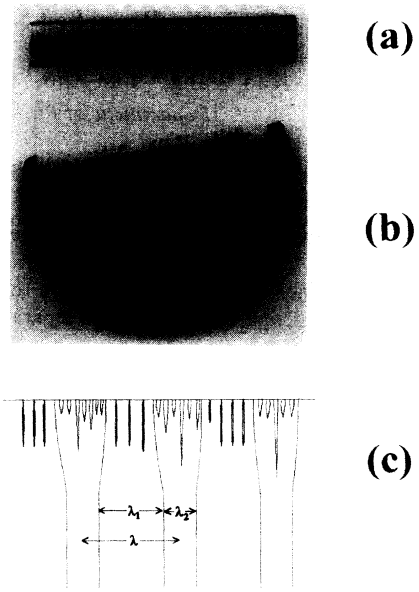

FIG. 3. Side views of unbranched and branched columns: (a) unbranched columns in the thinner part of the tube where the mean thickness is 18 μm, corresponding to the lattice structure in Fig. 1; (b) multiply branched columns with side structure between neighboring columns as observed in the wider part of the tube; the center thickness is 85 μm. The structure shown in (b) corresponds to the structure in Fig. 2 viewed from the side. (c) A sketch illustrating the geometry determined from (b).

plates is estimated to be less than 2 μm, determined by the thickness of the layer of glue holding the plates together. We found that when L increases, both the characteristic size of the column and the distance between columns increase. Furthermore, the circular cross section in Fig. 1 changes to a noncircular one at larger separation of cell thickness. Figure 2 is such a pattern in a cell of thickness $L = 25$ μm and an applied field of 300 G. It differs from the one in Fig. 1 not only by the characteristic size of each cross section and the distance between the two neighbors but also the actual structures themselves. The pattern in Fig. 2 represents a tree type structure with split branches (multiple bifurcations). We confirmed this by changing the focus of the microscope at different levels. When we slightly increase the distance from the object so as to focus at a higher level, one single object is seen to split into several separate ones.

One can argue that the periodic structure observed is simply due to the balance between the field energy term, which tries to elongate columns thus reducing the distance λ between them due to the volume conservation of the aggregates, and the repulsion between columns that favor the increase of λ. From this argument, Lemaire, Grasseli, and Bossis [5] assumed that in their magnetic suspension formed of micronic polystyrene particles surface tension is unimportant. However, we believe that the presence of interfacial tension between the phases plays an important role.

In order to further understand the difference between the structures in Figs. 1 and 2, we use a type C cell to view these structures from the side. Figure 3(a) shows the periodic columns in the thinner limit. We can see that the discrete phase does not wet the glass. Figure 3(b) shows the structure of a thicker layer. The branched structure at an end is clearly visible. Figure 3(c) is a sketch illustrating the geometry determined from Fig. 3(b). The magnetic fields in Figs. 3(a) and 3(b) are parallel to the axes of columns.

In 1986, a theory [6] predicted the scaling relation between λ and L as $\lambda \propto L^{1/3}$ from linear instability analysis. Bacri and Salin's result [3] was cited to support their prediction. We have measured the structure period λ as a function of cell thickness, L. Both type A and type B cells are used. We plot λ as a function of mean distance L from different subregions. The result from the type A cell is no different from the data taken from the type B cell. The results from type B cells are plotted in Fig. 4. Dots are the data from one kind of type B cell with a wedge angle of 0.06° and the triangles are from another type B cell with a wedge angle of 0.3°. The two points from the larger cell (circles) overlap well with the data from the smaller cell (triangles) in the region where the thicknesses from both cells are equal. In our thickness range we did not find the 1/3 scaling law as predicted by the theory in Ref. [6]. We noticed that if we plot λ versus L^{α} as in Ref. [6], the plot is not sensitive to α at all. In this plot α can be anywhere between $\frac{1}{3}$ to $\frac{3}{4}$. If we plot $\log\lambda$ versus $\log L$ the slope, or the scaling ex-

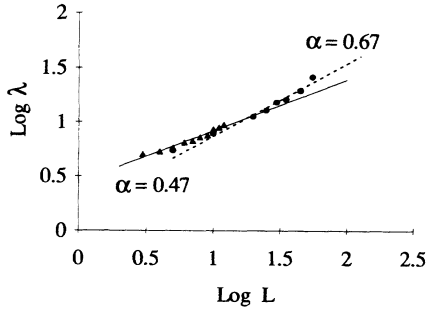

FIG. 4. The periodicity λ of columns scales with the thickness L of the sample cell. The scaling exponent is $\frac{1}{2}$ at small L and crosses over the $\frac{2}{3}$ at large L.

ponent, can be fitted unambiguously from a value around $\frac{1}{2}$ in the thin limit to $\frac{2}{3}$ in the thick limit. Our results disagree with that of Lemaire, Grasseli, and Bossis [5] where they found that the scaling exponent was 1. We believe that our choice of fitting function better represents the data. The crossover between scaling exponents occurs in the interval $10 < L < 20$ μm. The crossover marks the change from an unbranched to a branched structure as illustrated in Figs. 1 to 3.

In order to understand the mechanism responsible for both the unbranched and branched tree-type structures observed, we studied the free energy of the system. Because the average size of an aggregate is on the order of a few microns or larger, Brownian motion is essentially nonexistent. Thus the entropy term connected with an aggregate's thermal motion is negligible in the expression of the volume density of energy of the system which includes four terms: $E = f_1(n_1,H)\lambda_1/\lambda + f_2(n_2,H)\lambda_2/\lambda + 2\sigma/\lambda + f_m$, where f_1 and f_2 are the energies associated with the diluted and the concentrated single column, respectively. λ_1 and λ_2 are the column widths for diluted and concentrated phases, respectively, with $\lambda_1 + \lambda_2 = \lambda$ as illustrated in Fig. 3(c). n_1 and n_2 are particle volume fractions in the two phases and H is the applied magnetic field. $2\sigma/\lambda$ is the wall energy density, σ being the effective interfacial tension between concentrated and dilute phase, arising from attractive dipole interaction among particles. We believe that this attraction is responsible for the initial agglomeration in the system. f_m is the demagnetizing energy of periodic columns that accounts for both the energy associated with fictitious charges on surfaces of a single column and repulsion between neighboring columns. When phase separation occurs, most of the particles are in the concentrated domains. Thus for simplicity we assume that the volume fraction in the concentrated phase is the densest packing. Because of the particle conservation law we have $n_2\lambda_2 = n\lambda$, where n is the original particle concentration in the homogeneous phase. Because n and n_2 are both fixed, λ_2/λ is fixed. From the assumption of closest packing in the dense phase, the density of magnetic particles in the diluted phase 1 can be taken as zero. Therefore the first term in the energy expression disappears and the second term is a constant at the fixed field. Considering the case that the period λ is much smaller than the separation of the slot, L, and omitting the constant terms, the resulting energy can be expressed in the following form [7]:

$$E = \frac{2\sigma}{\lambda} + \frac{M^2}{\pi^2 L} 4\lambda \sum_{n=1}^{\infty} \frac{\sin^2(\pi n \lambda_2/\lambda)}{n^3[1+\coth(\pi n L/\lambda)]} - 2\pi\langle M\rangle^2 . \tag{1}$$

In Eq. (1) the magnetization for diluted phase is assumed equal to zero and M is the magnetization in the concentrated phase. The second and the third terms are the explicit expression for f_m. We found that the energy in (1) does not have a minimum without the surface tension term. This may be contrasted with Lemaire, Grasseli, and Bossis' argument [5] about the unimportance of surface tension. The extreme of (1) at the fixed volume fraction of agglomerates gives the characteristic power law for the periodicity of concentrated domain distribution:

$$\lambda = \alpha(\lambda_0 L)^{1/2}, \tag{2}$$

where $\lambda_0 = \sigma/M^2$ is the characteristic magnetic length and α is a numerical constant equal to

$$\alpha = \pi \left[\int_0^{\infty} dy\, y \ln \left[1 + \frac{\cos^2(\pi Z/2)}{\sinh^2 y} \right] \right]^{1/2}, \tag{3}$$

where $Z = 1 - 2\lambda_2/\lambda$. By comparing between Eq. (2) and the scaling exponent obtained from the plot in Fig. 4, we know that the energy form in Eq. (1) can describe the experimental results only in the thin limit (but we still have $L > \lambda$), because we did not include the surface contribution coming from the branched tails. To account for the structures shown in Figs. 2 and 3(b), we need to include the term connected with branching. Furthermore, to correctly describe experimental results, one also needs to add energy terms associated with small branches appearing between big columns as shown in Figs. 3(b) and 3(c). Including all the tiny agglomerates, the total energy for the whole system can be expressed by [8]

$$\frac{e}{M^2} = \alpha_1 \frac{\lambda_0}{\lambda} + 2\alpha_2 \frac{y^2\lambda}{L} + 2\alpha_3 \frac{(\lambda_0\lambda)^{1/2}}{L} - 2\alpha_4 \frac{(\lambda_0\lambda)^{1/2}}{L} y , \tag{4}$$

where $y = 2^{-N/2}$, and N is the number of branches determined by the derivative of (4) with respect to y. α_i are positive numerical constants depending on the volume fraction of magnetic particles and the angle between branches. The first term in Eq. (4) is similar to that in Eq. (1) accounting for the wall energy of each column. The second term is the demagnetizing energy due to surface charges. The third and the fourth terms are associated with the branching energies for small structures

(shrubs) present between columns and that of the columns, respectively. The second term in (4) can be expressed explicitly as $\lambda[\lambda_2/\lambda(1+2\xi)]y^2/L\alpha_1$, where λ_2/λ is a constant as discussed above. ξ is the ratio of the distance between the neighboring siblings to the width of the parent column. So the new period now changes to $\lambda/[(1+2\xi)2^N]$. Branching causes the surface periodicity to assume a much lower value than the bulk's, thus considerably reducing the demagnetizing energy. If L is large enough, this decrease largely compensates the additional branching energy term, favoring the branched structure. This is the origin of the dangling structures (shrubs) between neighboring branched columns (trees).

From Eq. (4) the equilibrium number of branches is determined by $d/dy(e/M^2)=0$, giving $y^*=\alpha_4/2\alpha_2(\lambda_0/\lambda)^{1/2}$. Since $y<1$, branching starts to appear when period λ exceeds a critical value λ^* that is proportional to the characteristic magnetic length λ_0. From the Hamiltonian in this regime, the equilibrium periodicity of the structure (columns) is equal to

$$\lambda=(\alpha_1/\alpha_3)^{2/3}\lambda_0^{1/3}L^{2/3}. \quad (5)$$

Equation (5) describes the scaling exponent observed experimentally for larger L as shown in Fig. 4. The crossover from $\frac{1}{2}$ to $\frac{2}{3}$ is attributed to the formation of small branches and shrubs in the system.

It is worth mentioning here that a two-dimensional ferromagnet [9] placed in a thin slab bears some similarities with our system. The equilibrium domain width λ in a ferromagnetic thin film is found to scale with the slab thickness D to the 1/2 power. For D larger than a certain value, which is a function of the domain wall and the magnetostatic energies, the branching instability develops. In this case, the ground state consists of a periodic branched structure with the periodicity λ related to the thickness D as $\lambda \propto D^{2/3}$ [9]. Although the exponents are similar to our system in both thin and thick limits, the physical mechanism and consequences are rather different. The competition associated with formation of ferromagnetic domains arises from different interactions: short range exchange interaction aligning spins in a parallel direction, and the long range dipole interaction favoring domain structures to reduce the global field energy. While in our system all the energies, including the field energy, the repulsive energy between neighboring branches and columns, and the surface energy, arise from dipole interaction among the particles or aggregates. Competition between different versions of the dipole energy leads to the scaling laws observed. Furthermore, the total domain volume of each orientation in a ferromagnet is not conserved. In our ferrofluid sample the total volume of the agglomerates is constant if we take the concentration in the dilute phase as zero.

In conclusion, we observed the periodic lattice structure in quasi 2D geometry in a phase-separated magnetic colloid. The periodicity λ scales with the layer thickness of the sample. The scaling exponent was found both experimentally and theoretically to be $\frac{1}{2}$ in the limit of a thin layer and crosses over to $\frac{2}{3}$ in the thick limit. The crossover is due to the branching of columns and appearance of small dangling structures that form between neighboring columns. The scaling relation originates from near field and far field dipole interactions alone insofar as the interfacial tension is due to the near field dipole force.

We thank David Rutherford for allowing us to use his bidirectional parallel interface card and Kodak SV 6500 color video printer.

*To whom correspondence should be addressed.

[1] C. Kittel, Rev. Mod. Phys. **21**, 541 (1949).

[2] R. E. Rosensweig, *Ferrohydrodynamics* (Cambridge Univ. Press, Cambridge, 1985); R. E. Rosensweig, M. Zahn, and R. Schumovich, J. Magn. Magn. Mater. **39**, 127 (1983); A. Cebers, Chem. Eng. Commun. **67**, 69 (1988), and references therein; S. A. Langer, R. E. Goldstein, and D. P. Jackson, Phys. Rev. A **46**, 4894 (1992).

[3] J. C. Bacri and D. Salin, J. Phys. (Paris), Lett. **43**, L-771 (1982); R. E. Rosensweig and J. Popplewell, in *Electromagnetic Forces and Applications*, edited by J. Tani and T. Tagaki (Elsevier, Amsterdam, 1992), pp. 83–86.

[4] V. N. Podkorytov and D. A. Yablonskii, Sov. Phys. Solid State **25**, 634 (1983); M. Gabay and T. Garel, Phys. Rev. B **33**, 6281 (1986); W. A. Barker and G. A. Gehring, J. Phys. C **19**, 259 (1986).

[5] E. Lemaire, Y. Grasseli, and G. Bossis, J. Phys. II (France) **2**, 359 (1992).

[6] A. Cebers, Magnitnaya Gidrodinamika (in Russian) **4**, 132 (1986).

[7] A. Cebers, Magnitnaya Gidrodinamika (in Russian) **3**, 49 (1990).

[8] Detailed calculation will be published in the follow-up paper.

[9] J. Kaczer, Sov. Phys. JETP **19**, 1204 (1964).

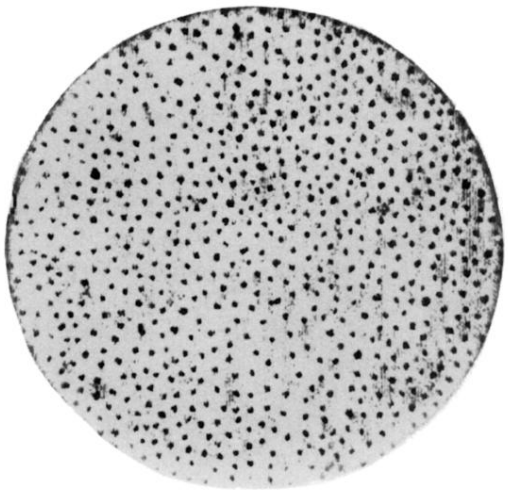

FIG. 1. Periodic lattice structure in a field of 300 G. The thickness L is less than 2 μm.

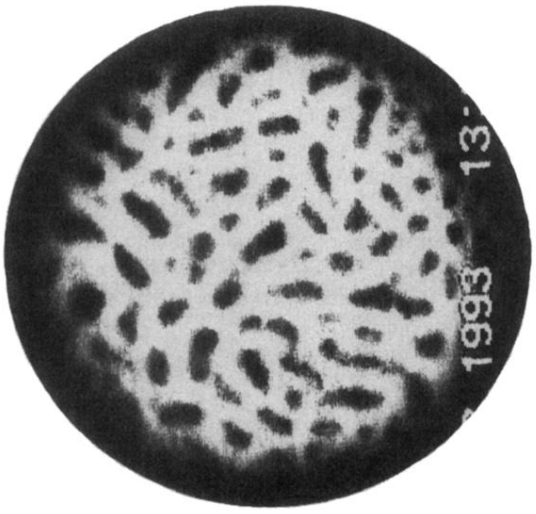

FIG. 2. Periodic pattern in a relatively thick cell. The thickness $L = 25$ μm. The cross sections are altered from their original circular geometry.

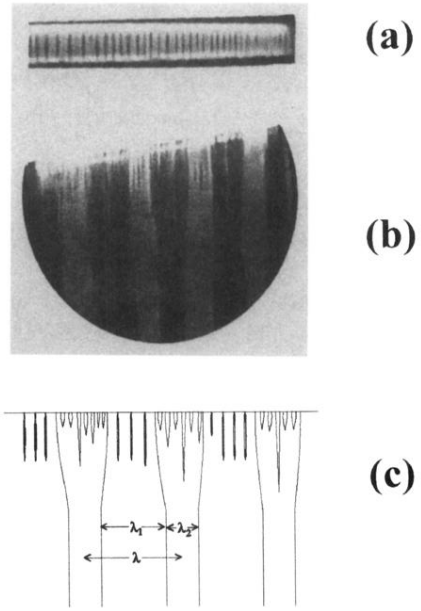

FIG. 3. Side views of unbranched and branched columns: (a) unbranched columns in the thinner part of the tube where the mean thickness is 18 μm, corresponding to the lattice structure in Fig. 1; (b) multiply branched columns with side structure between neighboring columns as observed in the wider part of the tube; the center thickness is 85 μm. The structure shown in (b) corresponds to the structure in Fig. 2 viewed from the side. (c) A sketch illustrating the geometry determined from (b).